Plant Biotechnology Journal

Plant Biotechnology Journal (2015), pp. 1–13 doi: 10.1111/pbi.12347

Virus-induced gene silencing of *Withania somnifera* squalene synthase negatively regulates sterol and defence-related genes resulting in reduced withanolides and biotic stress tolerance

Anup Kumar Singh[1,2], Varun Dwivedi[1,2], Avanish Rai[1,2], Shaifali Pal[1], Sajjalavarahalli Gangireddy Eswara Reddy[3], Dodaghatta Krishnarao Venkata Rao[2], Ajit Kumar Shasany[1] and Dinesh A. Nagegowda[1,2,*]

[1]*Biotechnology Division, CSIR-Central Institute of Medicinal and Aromatic Plants, Lucknow, India*

[2]*CSIR-Central Institute of Medicinal and Aromatic Plants Research Centre, Bangalore, India*

[3]*Hill Area Tea Science Division, Entomology Laboratory, CSIR-Institute of Himalayan Bioresource Technology, Palampur, Himachal Pradesh, India*

Received 27 October 2014;
revised 22 December 2014;
accepted 2 January 2015.
**Correspondence* (Tel 91 0522 2718554;
fax 91 0522 2719072;
email da.nagegowda@cimap.res.in)

Keywords: *Withania somnifera*, virus-induced gene silencing, squalene synthase, withanolides, transcriptional modulation, biotic stress.

Summary

Withania somnifera (L.) Dunal is an important Indian medicinal plant that produces withanolides, which are triterpenoid steroidal lactones having diverse biological activities. To enable fast and efficient functional characterization of genes in this slow-growing and difficult-to-transform plant, a virus-induced gene silencing (VIGS) was established by silencing *phytoene desaturase* (*PDS*) and *squalene synthase* (*SQS*). VIGS of the gene encoding SQS, which provides precursors for triterpenoids, resulted in significant reduction of squalene and withanolides, demonstrating its application in studying withanolides biosynthesis in *W. somnifera* leaves. A comprehensive analysis of gene expression and sterol pathway intermediates in *WsSQS*-vigs plants revealed transcriptional modulation with positive feedback regulation of mevalonate pathway genes, and negative feed-forward regulation of downstream sterol pathway genes including *DWF1* (*delta-24-sterol reductase*) and *CYP710A1* (*C-22-sterol desaturase*), resulting in significant reduction of sitosterol, campesterol and stigmasterol. However, there was little effect of *SQS* silencing on cholesterol, indicating the contribution of sitosterol, campesterol and stigmasterol, but not of cholesterol, towards withanolides formation. Branch-point oxidosqualene synthases in *WsSQS*-vigs plants exhibited differential regulation with reduced *CAS* (*cycloartenol synthase*) and cycloartenol, and induced *BAS* (β-*amyrin synthase*) and β-amyrin. Moreover, *SQS* silencing also led to the down-regulation of *brassinosteroid-6-oxidase-2* (*BR6OX2*), *pathogenesis-related* (*PR*) and *nonexpressor of PR* (*NPR*) genes, resulting in reduced tolerance to bacterial and fungal infection as well as to insect feeding. Taken together, *SQS* silencing negatively regulated sterol and defence-related genes leading to reduced phytosterols, withanolides and biotic stress tolerance, thus implicating the application of VIGS for functional analysis of genes related to withanolides formation in *W. somnifera* leaves.

Introduction

Withania somnifera (L.) Dunal, a member of Solanaceae family, commonly known as Ashwagandha, is a plant of high repute for thousands of years in Ayurveda. Its various medicinal properties are attributed to the presence of naturally occurring triterpenoid steroidal lactones collectively termed as withanolides (Mirjalili *et al.*, 2009). Antitumour, anti-inflammation, cardioprotective and neuroprotective properties are some of the major pharmacological activities reported for *W. somnifera* extracts (Mirjalili *et al.*, 2009; Sehgal *et al.*, 2012). So far more than 40 withanolides have been isolated from this plant in which withaferin A and withanolide D have been reported to inhibit angiogenesis, Notch-1 and NFκB in cancer cells and induce apoptosis in breast cancer cells (Hahm *et al.*, 2011; Kaileh *et al.*, 2007; Koduru *et al.*, 2010). Despite the importance of withanolides, their application is still limited owing to their low accumulation (0.001%–0.5% dry weights) in the plant and challenging nature of pure compound isolation from complex mixture. This can be overcome by metabolic engineering of plants, cell cultures or heterologous microbial systems. However, to achieve this, it warrants a thorough knowledge of the biosynthetic genes and regulatory mechanisms involved in the formation of withanolides. Current knowledge of withanolides biosynthetic pathways is limited due

Please cite this article as: Singh, A.K., Dwivedi, V., Rai, A., Pal, S., Reddy, S.G.E., Rao, D.K.V., Shasany, A.K. and Nagegowda, D.A. (2015) Virus-induced gene silencing of *Withania somnifera* squalene synthase negatively regulates sterol and defence-related genes resulting in reduced withanolides and biotic stress tolerance. *Plant Biotechnol. J.*, doi: 10.1111/pbi.12347

to the lack of available genome sequence data and more importantly due to nonavailability of reliable and technically undemanding methods for functional gene assays in *W. somnifera*.

Withanolides are C_{28} steroidal lactones in which C_{22} and C_{26} are oxidized to form lactone ring. Like sterols, withanolides are derived from the common 5-carbon precursor, isopentenyl diphosphate (IPP) and its isomer dimethylallyl diphosphate (DMAPP), which are formed via either the cytosolic mevalonate (MVA) pathway or the plastidial methylerythritol phosphate (MEP) pathway (cf. Nagegowda, 2010; Figure 1). While the MVA pathway provides precursors for sesqui-, tri- and polyterpenes, the MEP pathway is responsible for supplying the precursors for mono-, di-, tetra- and polyterpenes (cf. Nagegowda, 2010). Condensation of two IPP units with a DMAPP unit in 'head-to-tail' fashion forms C_{15} farnesyl diphosphate synthase (FPP), two of which fuse 'head-to-head' to generate the linear C30 triterpenoid precursor, squalene in a reaction catalysed by squalene synthase (SQS). Subsequently, 2,3-oxidosqualene, formed from squalene by squalene epoxidase (SQE), undergoes cyclization by specific oxidosqualene cyclases (OSCs) to tetra- or pentacyclic structures (Phillips *et al.*, 2006). Cycloartenol synthase (CAS) converts 2,3-oxidosqualene to cycloartenol, which acts as the precursor for all sterols. It is proposed that sterols synthesized *via* the universal sterol pathway act as precursors for the biosynthesis of withanolides (Figure 1). These precursors may undergo various biochemical transformations such as hydroxylation and glycosylation reactions leading to the formation of various withanolides (Singh *et al.*, 2014).

In the postgenomic era, virus-induced gene silencing (VIGS) has emerged as a powerful reverse genetic tool to study the function of genes. VIGS using TRV vector system has been demonstrated in various Solanaceous species including model plants tobacco and a number of agriculturally important plant species such as tomato, potato and egg plant (Faivre-Rampant *et al.*, 2004; Liu *et al.*, 2002a,b, 2012). However, VIGS in medicinally important Solanaceous plants is limited with only example of *Hyoscyamus niger* (black henbane), in which VIGS has been utilized to study a gene encoding cytochrome P450 involved in tropane alkaloid biosynthesis (Li *et al.*, 2006). SQS, a key enzyme that catalyses the first committed step, plays a crucial role in redirecting the carbon flux from the central isoprenoid pathway towards triterpenoid biosynthesis (Devarenne *et al.*, 2002; Wentzinger *et al.*, 2002). Although SQS has also been shown to play regulatory role in triterpenoid biosynthesis and stress tolerance (Lee *et al.*, 2004; Seo *et al.*, 2005; Wang *et al.*, 2012b; Wentzinger *et al.*, 2002), a comprehensive analysis of the effect of squalene depletion on sterol and defence-related genes, pathway intermediates and biotic stress was missing.

In this study, to develop a VIGS approach and to explore its utility for functional analysis of genes related to withanolides biosynthesis in *W. somnifera* leaves, genes encoding phytoene desaturase (PDS) and SQS were successfully down-regulated by VIGS. *WsSQS*-vigs led to significant reduction of individual as well as total withanolides in leaves. In addition, a thorough analysis of the effect of *WsSQS*-vigs on transcription of early terpenoid MVA pathway, triterpenoid pathway and defence-related genes was carried out. Subsequently, the effect of *WsSQS*-vigs on triterpenoid pathway intermediates and biotic stress tolerance was investigated.

Results

Optimization of VIGS in *Withania somnifera*

To establish VIGS in *W. somnifera*, first we tested the infectivity of TRV in *W. somnifera* by infiltrating the leaves of four-leaf-staged plants with 1 : 1 mixture of *Agrobacterium* cultures harbouring pTRV1 and pTRV2 vectors. The spread of virus was confirmed by reverse-transcriptase polymerase chain reaction (RT-PCR) using TRV1 and TRV2 specific primers with cDNA prepared from newly emerged leaves. While there was no amplification in control plants, all treated plants showed amplicons corresponding to TRV1 and TRV2, demonstrating that TRV vectors can be used for VIGS in *W. somnifera* (Figure S1). As *PDS* is widely used as a marker in VIGS, a 493-bp *PDS* fragment from *W. somnifera* leaf cDNA was cloned into *Xba*I and *Xho*I sites of pTRV2 VIGS vector, and the resulting TRV:*WsPDS* construct (Figure S2) was transformed into *Agrobacterium tumefaciens*. To optimize gene silencing, syringe and vacuum infiltration of leaves of 4-leaf-staged seedlings and vacuum infiltration of 1-week-old seed sprouts were performed using *Agrobacteria* cultures containing TRV1 and TRV:*WsPDS* constructs. However, vacuum-infiltrated seedlings and sprouts showed low survival rate, and those that survived did not yield a photobleached phenotype. In syringe-infiltrated seedlings, the photobleached phenotype became apparent both in infiltrated leaves as well as in newly emerging leaves 17–20 days postinfiltration (dpi). The phenotype ranged from mild photobleaching having varied patches distributed on the leaf surface to strong uniform photobleaching in the entire leaf (Figure 2a,b). In most occasions, leaves showed a mild phenotype as albino and green patches. Many plants with VIGS response exhibited a photobleached phenotype in newly emerging leaves up to 3–4 months (Figure 2a). Subsequent transcript analysis by real-time qPCR in corresponding leaves showed a significant decrease in *PDS* mRNA levels ranging from 49% to 94% in tissues of *WsPDS*-vigs plants when compared with EV (Figure 2b). The frequency and effectiveness of VIGS in *W. somnifera* were found to be 49% and 34%, respectively (Figure S3).

Silencing of *WsSQS* reduces the accumulation of squalene and withanolides

To examine the potential of VIGS approach in studying withanolides biosynthesis in *W. somnifera* leaves, gene encoding SQS, which provides precursor for phytosterols and withanolides, was silenced. *WsSQS*-vigs plants generally exhibited stunted growth compared with EV control plants, and leaves exhibiting typical viral infection phenotype such as slight curling were collected for analysis (Figure S4). Care was taken to collect leaves of similar developmental stages in both *WsSQS*-vigs and EV plants. *WsSQS*-vigs leaves showed reduced accumulation of *SQS* transcripts in all three samples compared with leaves of EV plants (Figure 3a). The reduction in *SQS* mRNA expression ranged from approximately 87% to 90%, suggesting that the target gene silencing can be carried out without the need of a visible marker. To determine the effect of *WsSQS* silencing on squalene accumulation, pooled leaf tissues from 4 to 6 *WsSQS*-vigs and EV plants were collected, dried and extracted with methanol. Analysis of methanolic extracts revealed a significant reduction of squalene content (approximately 54%–60%) in *WsSQS*-vigs samples compared with EV (Figures 3b and S5). Next, to investigate the *WsSQS*-silencing effect on withanolides accumulation, major withanolides were analysed by high-performance liquid chromatography

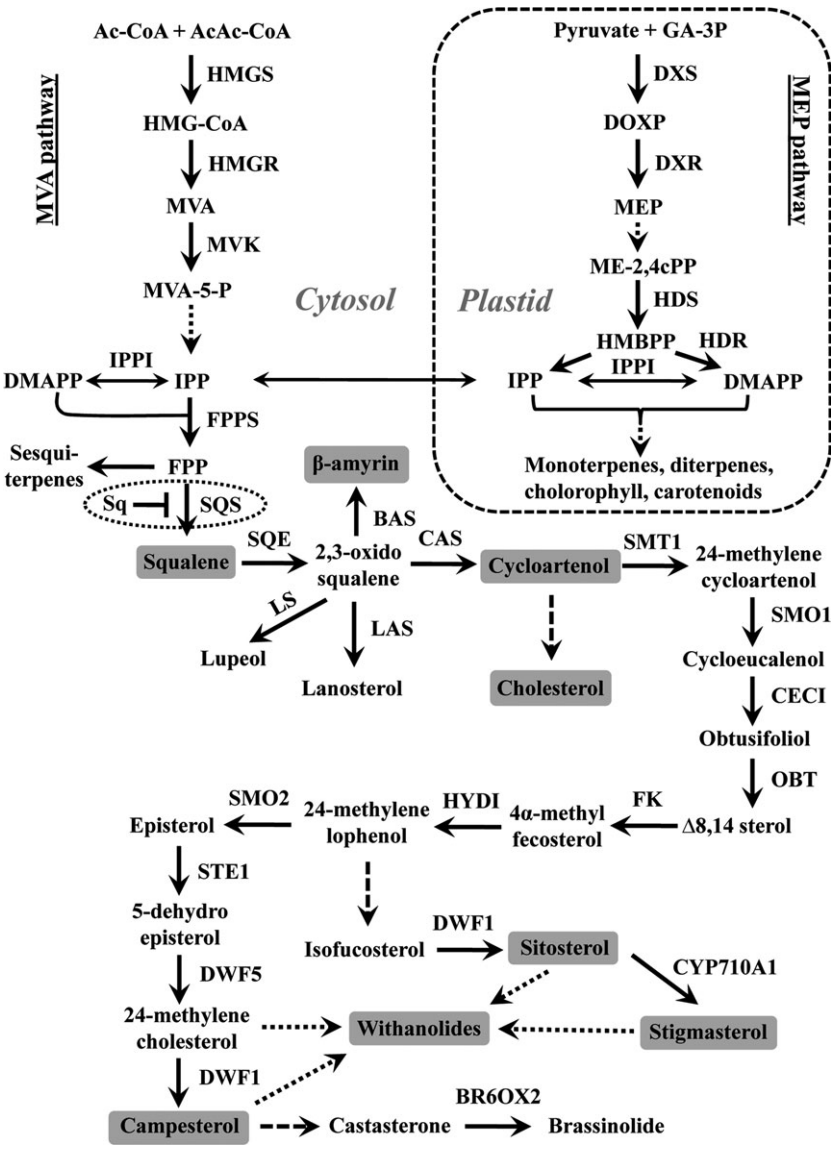

Figure 1 Simplified view of isoprenoid biosynthesis in plants. Solid arrows indicate single-step reactions, dashed arrows denote several steps, dotted arrows represent unidentified steps, and the double arrow between cytosolic and plastid compartments indicates metabolic crosstalk between them. Metabolites that are quantified in this study are shown in grey test box. Ac-CoA, acetyl CoA; AcAc-CoA, acetoacetyl CoA; BAS, β-amyrin synthase; BR6OX2, brassinosteroid-6-oxidase 2; CAS, cycloartenol synthase; CECI, cycloeucalenol cycloisomerase; CYP710A1, C-22 sterol desaturase; DMAPP, dimethylallyl diphosphate; DOXP, 1-deoxy-D-xylulose 5-phosphate; DWF1, delta-24 sterol reductase; DWF5, sterol delta-7 reductase; DXR, 1-deoxy-D-xylulose 5-phosphate reductoisomerase; DXS, 1-deoxy-D-xylulose-5-phosphate synthase; FK, delta 14-sterol reductase; FPP, farnesyl diphosphate; FPPS, FPP synthase; GA-3P, glyceraldehyde 3-phosphate; HDR, 4-hydroxy-3-methylbut-2-enyldiphosphate reductase; HDS, 4-hydroxy-3-methylbut-2-enyldiphosphate synthase; HMBPP, 4-hydroxy-3-methylbut-2-enyl diphosphate reductase; HMG-CoA, 3-hydroxy-3-methylglutaryl-CoA; HMGR, HMG-CoA reductase; HMGS, HMG-CoA synthase; HYDI, C-7,8 sterol isomerase; IPP, isopentenyl diphosphate; IPPI, isopentenyl diphosphate isomerase; LAS, lanosterol synthase; LS, lupeol synthase; ME-2,4cPP, 2-*C*-methyl-D-erythritol 2, 4-cyclodiphosphate synthase; MEP, 2-*C*-methyl-D-erythritol 4-phosphate; MVA, mevalonate; MVA-5-P, 5-phosphomevalonate; MK, mevalonate kinase; OBT, obtusifoliol 14-demethylase; SMO1, sterol-4α-methyl oxidase 1; SMO2, sterol-4α-methyl oxidase 2; SMT1, sterol methyltransferase 1; SQE, squalene monooxygenase/epoxidase; Sq, squalestatin; SQS, squalene synthase; STE1, C-5 sterol desaturase.

(HPLC) using *WsSQS*-vigs and EV leaves. It was observed that there was a drastic reduction of withanolides accumulation in *WsSQS*-vigs samples compared with EV plants as evident from HPLC chromatograms (Figure 4a). About 54% reduction in total withanolides content was observed in *WsSQS*-vigs leaves compared with control (Figure 4b). Among the individual withanolides, withaferin A, the major withanolide present in leaves, exhibited the highest decline with approximately 64%, followed by withanolide IV (approximately 47.5%) and withanolide A (approximately 37%) (Figure 4b). Further, to validate the results obtained in *SQS*-silenced tissues, *W. somnifera* leaves were infiltrated with 0.5 μM of squalestatin, a specific inhibitor of SQS. The reduction of squalene and withanolides due to *SQS* silencing by VIGS was similar to the results obtained from

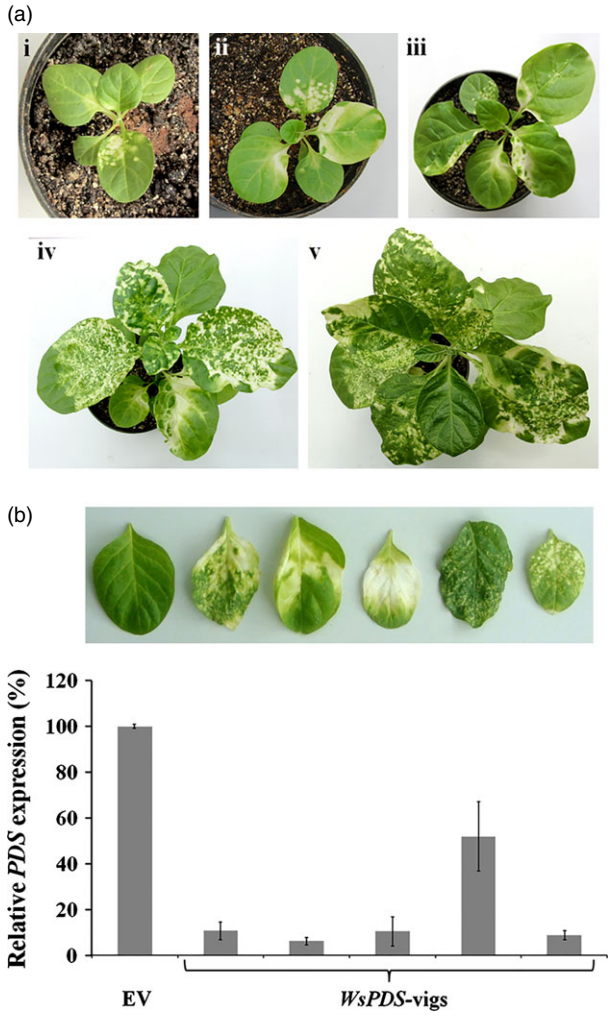

Figure 2 Tobacco rattle virus (TRV)-mediated silencing of *PDS* in *Withania somnifera*. (a) Phenotypes of *W. somnifera* plant infiltrated with *WsPDS*-vigs construct at different dpi. (i) 32 dpi, (ii) 37 dpi, (iii) 50 dpi, (iv) 61 dpi, (v) 73 dpi. (b) *Withania somnifera* leaves exhibiting varying phenotypes in different *WsPDS*-vigs leaves at 40 dpi in comparison (top panel) and the corresponding mRNA expression levels of *PDS* analysed by real-time qPCR (bottom panel). The expression levels of *PDS* transcripts were normalized to *18S rRNA* and represented as % reduction in comparison with EV, which was set to 1. Data are means ± SE of six technical replicates.

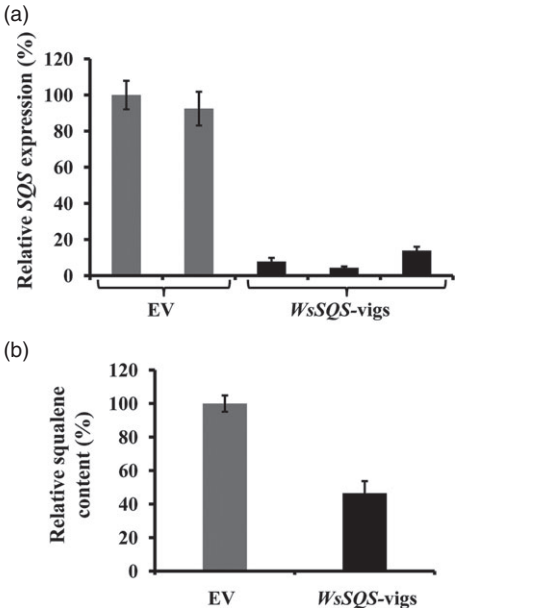

Figure 3 Tobacco rattle virus (TRV)-mediated silencing of *SQS* in *Withania somnifera* leaves. (a) Real-time qPCR analysis showing relative expression levels of *SQS* gene in systemic leaves of *W. somnifera* plants infiltrated with TRV (EV) and TRV:*WsSQS* (*WsSQS*-vigs). The expression levels of *WsSQS* transcript were normalized to *18S rRNA*. Data are means ± SE of six technical replicates. (b) Relative quantification of the squalene content of leaf extracts of *W. somnifera* plants infiltrated with TRV and TRV:*WsSQS*. Squalene was extracted from pooled tissue of systemic leaves of infiltrated plants and analysed by TLC. The corresponding squalene spots on TLC plates visualized after iodine staining were quantified by ImageJ analysis. Data are means ± SE of two independent pooled tissues of EV and *WsSQS*-vigs plants. Each pooled tissue consisted of leaves from three individual plants. TLC analysis for each sample was carried out in duplicate.

squalestatin-treated leaves (Figure S6), demonstrating the effectiveness of VIGS for functional studies of genes involved in withanolides biosynthesis in *W. somnifera*.

Silencing of *WsSQS* imparts positive feedback and negative feed-forward regulation of sterol pathway genes

It has been reported that inhibition of SQS in tobacco BY2 cells results in depletion of endogenous sterols, which brings about positive feedback regulation of HMGR both at mRNA and protein level (Wentzinger *et al.*, 2002). However, it is not clear whether blocking of SQS affects the expression of other sterol pathway genes. To validate this, mRNA levels of genes both upstream and downstream of SQS were analysed by real-time qPCR in *WsSQS*-silenced and control samples of *W. somnifera* (Figure 5). It was observed that all analysed genes of MVA pathway upstream of SQS were up-regulated in *WsSQS*-vigs samples compared with control. Both *HMGR1* and *HMHGR2* exhibited the highest level (approximately fivefold) of up-regulation followed by *HMGS*, *MK* and *FPPS* (Figure 5). Interestingly, most of the analysed sterol pathway genes (*SQE*, *SMT1*, *CECI*, *OBT*, *FK*, *HYDI*, *STE1*, *DWF1*, *DWF5*, *CYP710A1*) downstream of SQS were significantly down-regulated in response to *SQS* silencing (Figure 5). The degree of down-regulation ranged from 44% for *OBT* to 76% for *DWF5*. As it was reported that both MVA and MEP pathways contribute to the formation of sterols and withanolides (Chaurasiya *et al.*, 2012; Hasunuma *et al.*, 2008; Singh *et al.*, 2014), the effect of *SQS* silencing on the expression of MEP pathway genes (*DXS*, *DXR*, *HDS* and *HDR*) was analysed. Unlike sterol pathway genes, there was no significant effect on the expression of all four analysed genes (Figure 5). Moreover, chlorophyll and carotenoid contents were unaffected in *WsSQS*-vigs plants compared with EV (Figure S7). Squalestatin-treated *W. somnifera* leaves showed similar trend of transcript levels for *DXR*, *HMGS, HMGR*, *SQE and CYP710A1* (Figure S8) to that of *WsSQS*-vigs leaves, further confirming the results obtained in VIGS of *WsSQS*.

WsSQS silencing differentially regulates the expression of genes encoding branch-point oxidosqualene synthases

To determine the effect of *SQS* silencing on mRNA expression of branch-point oxidosqualene synthase genes, qPCR analysis and

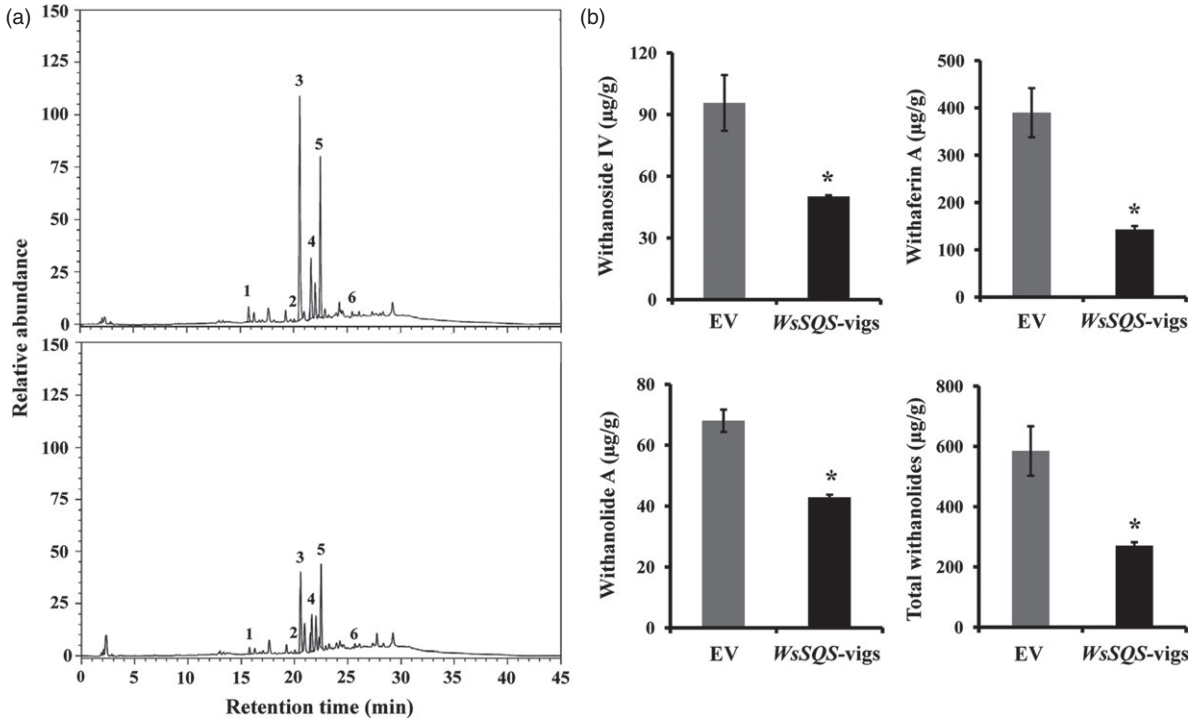

Figure 4 Withanolides profiles of EV and *WsSQS*-vigs leaves. (a) Representative high-performance liquid chromatography (HPLC) chromatograms of samples from EV (top panel) and *WsSQS*-vigs (bottom panel) leaves showing relative abundance of different withanolides. 1, withanolide IV; 2, withanolide V; 3, withaferin A; 4, 12-deoxywithastramonolide; 5, withanolide A; 6, withanolide B. (b) Relative quantification of withanolide IV, withaferin A, withanolide A and total withanolides in EV and *WsSQS*-vigs leaves. Data are means ± SE of four independent pooled tissues of EV and *WsSQS*-vigs plants. Each pooled tissue consisted of leaves from three individual plants. HPLC analysis for each sample was carried out in triplicate. Asterisks indicate a significant difference from the control (Student's *t*-test; $*P < 0.05$).

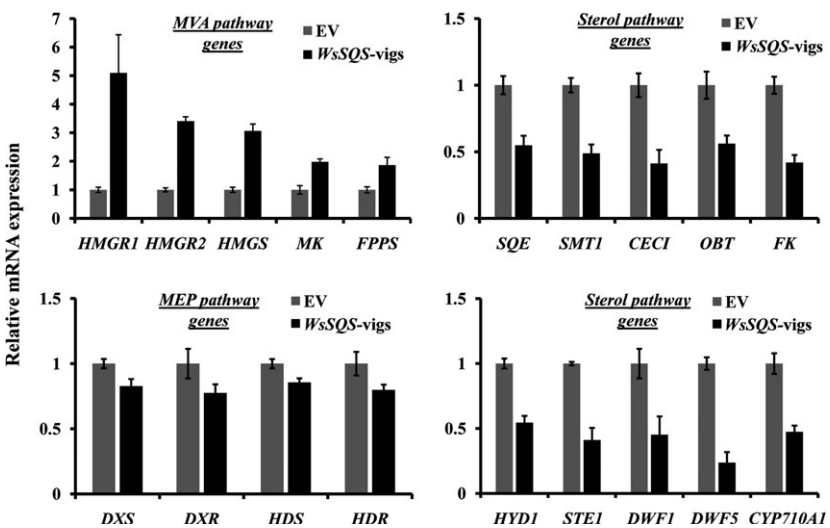

Figure 5 Real-time qPCR analysis showing relative expression levels of mevalonate (MVA), methylerythritol phosphate (MEP) and sterol pathway genes in EV and *WsSQS*-vigs leaves. Data are means ± SE of six technical replicates using cDNA prepared from EV and *WsSQS*-vigs plants. Sample size, $n = 2$ for EV and $n = 3$ for *WsSQS*-vigs. Expression levels of these genes were normalized to *18S rRNA* and are represented in comparison with EV control. EV value was set to 1 to calculate relative expression levels.

quantification of metabolites arising from those branch points was carried out in *WsSQS*-vigs and EV leaves. It was observed that similar to other genes of phytosterol biosynthesis, *CAS* was significantly down-regulated (56%) in *WsSQS*-vigs leaves (Figure 6a). Further, there was reduced accumulation of cycloartenol in *WsSQS*-vigs plants (65%) (Figure 6a). While the gene encoding β-amyrin synthase (BAS), which provides precursor for pentacyclic triterpenes, was up-regulated (approximately 3.8-fold) with a significant increase of β-amyrin content (approximately 23%) (Figures 6b and S9), the other two branch-point genes *LAS* and

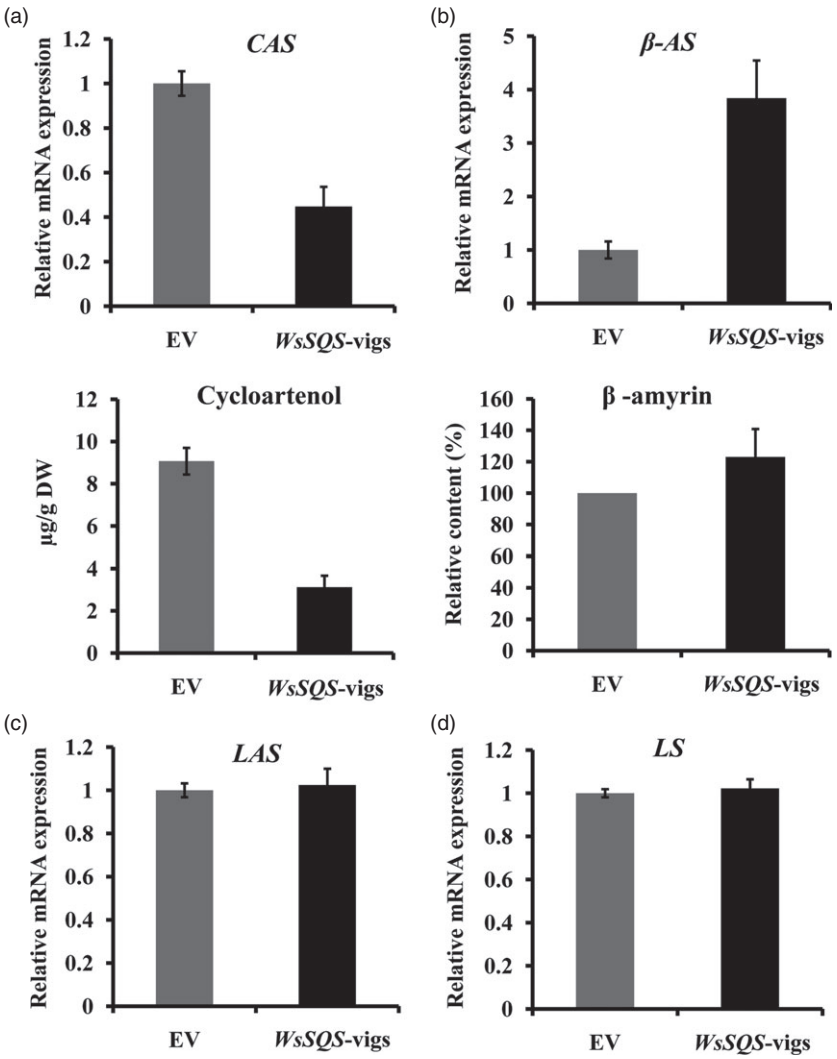

Figure 6 Effect of *WsSQS*-vigs on branch-point oxidosqualene cyclases. (a) Relative expression level of *CAS* (top graph) and corresponding cycloartenol content (bottom graph) in EV and *WsSQS*-vigs leaves. Cycloartenol was analysed and quantified by gas chromatography (GC). (b) Relative expression of *BAS* (top graph) and β-amyrin content (bottom graph) in EV and *WsSQS*-vigs leaves. β-amyrin content extracted from pooled tissues of EV and *WsSQS*-vigs leaves is represented. Relative expression profiling of *LAS* (c) and *LS* (d) genes in EV and *WsSQS*-vigs leaves. EV value was set to 1 to calculate relative expression levels. Data are means ± SE of six technical replicates using cDNA prepared from EV and *WsSQS*-vigs plants. Sample size, $n = 2$ for EV and $n = 3$ for *WsSQS*-vigs. Data for cycloartenol are means ± SE of two independent pooled tissues of EV and *WsSQS*-vigs plants. Each pooled tissue comprised leaves from six individual plants. GC analysis was carried out for each sample in triplicate. β-amyrin was quantified by TLC using the same samples mentioned in Figure 3. TLC analysis for each sample was carried out in duplicate.

LS were not affected by *WsSQS* silencing (Figure 6c,d). Expression of *CAS*, *BAS*, and *LAS* and β-amyrin content in squalestatin-treated leaves was similar to that of *WsSQS*-vigs plants (Figures S8 and S10). These results indicated some differential regulation of branch-point genes in response to *WsSQS* silencing, resulting in differential flux allocation towards products arising from branch points.

WsSQS-vigs reduced the accumulation of phytosterols

As *SQS* silencing resulted in reduced levels of withanolides (derivatives of phytosterols) and down-regulation of sterol pathway genes, individual phytosterol levels were determined by gas chromatography (GC) analysis in *WsSQS*-vigs plants. Quantification of results from GC analysis indicated a significant decline in total sterol content (approximately 16%) of *WsSQS*-vigs leaves in comparison with EV (Figure 7e). Among individual sterols, the extent of their reduction in *WsSQS*-vigs leaves ranged from 15% to 26%. Both sitosterol (Figure 7a) and campesterol (Figure 7c) exhibited a similar decline as that of total sterols with a decrease of 15% and 16%, respectively, in *WsSQS*-vigs leaves. However, the reduction of stigmasterol in *WsSQS*-vigs leaves was much more prominent than that of the other two phytosterols with a decrease of 26% (Figure 7b). There was no significant decline in cholesterol content in *WsSQS*-vigs leaves (Figure 7d).

WsSQS silencing negatively affects the expression of defence-responsive *PR, NPR and BR6OX2* genes

It has been reported that down-regulation of *SQS* and knockout of *AtCYP710A1* in *Arabidopsis* compromise plant innate immunity against bacterial pathogens (Wang *et al.*, 2012b). As we observed down-regulation of *CYP710A1* involved in stigmasterol biosynthesis and reduced phytosterols in *WsSQS*-vigs plants (Figure 5), we were tempted to check the effect of down-regulation of *SQS* and *CYP710A1* on the expression of pathogenesis-related (*PR*) genes. Therefore, the mRNA levels of both salicylic acid (SA)- and jasmonic acid (JA)-dependent *PR* genes were determined in *WsSQS*-vigs and EV plants, which showed drastic reduction of both SA-dependent *PR1* (46%) and *PR5* (76%), and JA-dependent *PR3* (50%) transcripts in *SQS*-silenced samples (Figure 8a). As it was reported that *PR* gene expression is dependent on nonexpressor of PR (NPR) genes (Fan and Dong, 2002) as well as brassinolide (Divi *et al.*, 2010), the expression of genes encoding NPR1 and NPR3, and BR6OX2 (which catalyses the conversion of castasterone to brassinolide) was analysed in both *WsSQS*-vigs and EV leaves. It was observed that both *BR6OX2* and *NPR* genes exhibited significant reduction in their mRNA levels in *WsSQS*-vigs leaves. While *BR6OX2* showed 54% reduction, *NPR1* and *NPR3* exhibited 45% and 81% reduction,

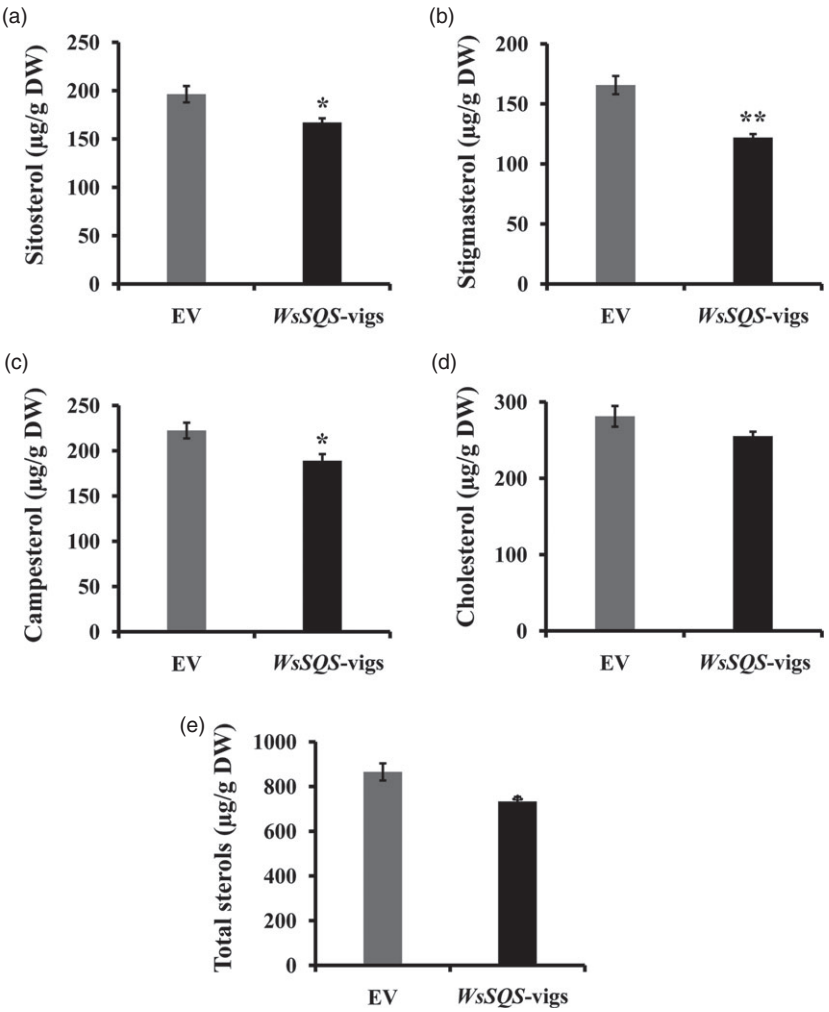

Figure 7 Phytosterol composition of EV and *WsSQS*-vigs leaves of *Withania somnifera.* Phytosterols were extracted from dried leaves and quantified by gas chromatography (GC) analysis. Graphs represent the µg/g composition of sitosterol (a), stigmasterol (b), campesterol (c), cholesterol (d), and total sterols (e) in EV and *WsSQS*-vigs leaves of *W. somnifera*. Data are means ± SE of two independent pooled tissues of EV and *WsSQS*-vigs plants. Each pooled tissue comprised leaves from six individual plants. GC analysis was carried out for each sample in triplicate. Asterisks indicate a significant difference from the control (Student's *t*-test; $^{**}P < 0.01$ and $^{*}P < 0.05$).

respectively (Figure 8b), indicating a link between the level of endogenous sterols, brassinolide and NPR-dependent *PR* gene expression.

WsSQS-vigs leaves exhibit reduced tolerance to bacterial and fungal pathogens

As silencing of *WsSQS* resulted in reduced sterol and withanolides content, and reduced defence-related gene expression, we checked the effect of biotic stress *WsSQS*-vigs leaves. Fully expanded first-pair leaves of *WsSQS*-vigs and EV leaves were infiltrated with *Pseudomonas syringae*. Extracts isolated from leaf discs of *P. syringae* infiltrated leaves at 4 dpi were used for bacterial growth assay. The results indicated that extracts from *WsSQS*-vigs samples supported significantly higher *P. syringae* multiplication than extracts from EV leaves (Figure 8c). In fungal infection assay with the necrotrophic pathogen *Botrytis cinerea*, *WsSQS*-vigs leaves started exhibiting mild disease symptoms compared with EV at 3 dpi (Figure 9a). However, at 4 dpi, *WsSQS*-vigs leaves developed severe disease symptoms and sustained more tissue damage than EV leaves (Figure 9a). *WsSQS*-vigs leaves were chlorotic or macerated, whereas leaves from control plants remained green with necrotic spots restricted to initial culture droplet area without much spreading of infection (Figure 9a). *WsSQS*-vigs leaves exhibited reduced resistance to *B. cinerea* infection, which was evident by a significant increase (approximately 2.45-fold) in diameter size of lesions compared with that of EV leaves (Figure 9b).

WsSQS-vigs leaves are susceptible to tobacco cutworm *Spodoptera litura*

To assess the effect of reduced phytosterols and withanolides in *WsSQS*-vigs leaves on insect feeding, a dual-choice feeding preference test was performed using tobacco cutworms (*Spodoptera litura*). Equal numbers (six each) of second-instar larvae were placed on similar-sized leaves placed in a Petri dish from *WsSQS*-vigs and EV plants. After 12 h, most *S. litura* larvae preferred eating *SQS*-silenced leaves rather than control leaves (Figure 9c). There was approximately 2.7-fold higher consumption of leaves in *WsSQS*-vigs samples than EV (Figure 9d). Also, preference index (PI) determination showed a higher preference of tobacco cutworm larvae for *WsSQS*-vigs leaves (PI = 1.4) compared with EV (PI = 1.0) (Figure 9e).

Discussion

In this work, we have demonstrated that VIGS could be effectively used to down-regulate genes in *W. somnifera* by silencing *PDS* and *SQS* genes (Figures 2 and 3). Although different methods have been used for introducing pTRV1/pTRV2 plasmids through *Agrobacterium*-mediated infection, including vacuum (Hileman

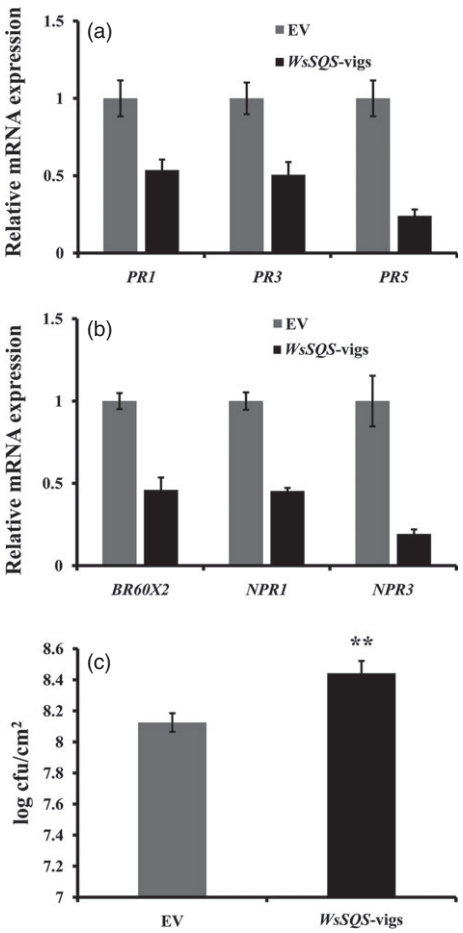

Figure 8 Effect of *WsSQS*-vigs on defence-related genes in *Withania somnifera*. Relative expression levels of *PR* genes (a) and *BR6OX2* and *NPR* genes (b) in EV and *WsSQS*-vigs leaves. EV value was set to 1 to calculate relative expression levels. Data are means ± SE of six technical replicates using cDNA prepared from EV and *WsSQS*-vigs plants. Sample size, $n = 2$ for EV and $n = 3$ for *WsSQS*-vigs. (c) Bacterial growth assay with *Pseudomonas syringae* on EV and *WsSQS*-vigs leaves. First pair of leaves at 30 dpi having viral infection phenotype was infiltrated with *P. syringae*. Bacterial growth at 4 dpi was obtained by plating serial dilutions of leaf extracts from EV and *WsSQS*-vigs. Data represent mean ± SE of two independent experiments representing four biological replicates. Asterisks indicate a significant difference from the control (Student's *t*-test; $^{**}P < 0.01$).

et al., 2005), syringe (Ratcliff *et al.*, 2001) and sprout infiltration (Yan *et al.*, 2012), only syringe infiltration of seedlings yielded reliable and consistent silencing of *WsPDS* with 90%–95% survival rate. However, in our results, there was very little survival rate of seedlings and sprouts after vacuum infiltration, which might be due to the injury inflicted by vacuum on the fragile shoot of seedlings and radicle of sprouts. The frequency (approximately 47%) and efficiency (approximately 33%) of gene silencing were comparable to the frequency and efficiency obtained in other Solanaceous plants (Liu *et al.*, 2012; Senthil-Kumar *et al.*, 2007). Also, the endogenous *W. somnifera PDS* was effectively silenced using heterologous *PDS* from *Nicotiana tabacum* (TRV:*NtPDS*) with similar efficiency to that of *TRV:WsPDS*, suggesting the use of heterologous sequences for silencing orthologue genes whose sequence information is not known in *W. somnifera* but present in other Solanaceae species (Figures S11 and S12). SQS is an important enzyme and acts as a regulatory step in the isoprenoid biosynthetic pathway, diverting carbon flow from the central isoprenoid pathway specifically towards sterol and triterpenoid biosynthesis (Devarenne *et al.*, 2002). Hence, to check the involvement of SQS in withanolides biosynthesis, VIGS approach was utilized to silence *SQS* in *W. somnifera*. Given that squalene is the first committed precursor for triterpenoid biosynthesis (Figure 1), *WsSQS*-vigs led to drastic reduction of both individual and total withanolides (Figure 4). Although SQS located high in the pathway is not the key enzyme for withanolides biosynthesis, silencing of *SQS* reduced the withanolides content due to the decreased availability of squalene (Figure 3), the common precursor of triterpenoids.

To obtain a comprehensive understanding of the effect of *SQS* silencing or SQS inhibition on pathway gene expression, we carried out qPCR analysis of several genes upstream and downstream of SQS. Our results present new evidence that *SQS* silencing or SQS inhibition leads to positive feedback and negative feed-forward regulation of sterol biosynthetic genes with up-regulation of MVA pathway genes located upstream of SQS and coordinated down-regulation of sterol pathway genes situated downstream of SQS (Figures 5 and S8). Up-regulation of *HMGR* was in agreement with a previous report in tobacco BY-2 cells in which SQS inhibition by squalestatin up-regulated both *HMGR* expression and activity (Wentzinger *et al.*, 2002). Also, it has been shown that *HMGR* expression and enzyme activity are regulated by SQS level and by sterol end product of the pathway (Ginzberg *et al.*, 2012; Holmberg *et al.*, 2002; Nes and Venkatramesh, 1999). In addition, there was significant up-regulation of other tested MVA pathway genes (*HMGS*, *MK*, *IPPI* and *FPPS*) albeit at a lesser level compared with *HMGR* in *SQS*-silenced plants (Figure 5). Reduction of transcript levels of genes downstream of SQS in *SQS*-silenced tissues indicates possible co-regulation of these genes with *SQS*. However, at this point, the precise relationship between *SQS* silencing and differential regulation of upstream and downstream genes is not clear and needs to be investigated further. It can be speculated that increased FPP pool in *SQS*-silenced plants could affect protein-prenylation-related signalling events thus activating unfolded protein response, which has been reported to be involved in regulating sterol biosynthetic genes (Martínez and Chrispeels, 2003). In the case of MEP pathway genes, there was no significant effect on their mRNA expression level with no apparent effect on chlorophyll and carotenoid content in *SQS*-silenced tissues (Figures 5 and S7), indicating that *SQS* silencing has little effect on the MEP pathway. As *SQS* silencing down-regulated *SQE* including *CAS* (one of the branch-point oxidosqualene synthases) resulting in reduced cycloartenol (Figure 6a), we were curious to know the expression of other OSCs, which function at the branch points and catalyse the cyclization of 2,3-oxidosqualene to provide precursors for various triterpenoids (Figure 1; Moses *et al.*, 2013). It was found that the mRNA accumulation of genes encoding LS and LAS was not affected, but interestingly, *BAS* mRNA levels were induced in *SQS*-silenced tissues with corresponding increase in β-amyrin content (Figure 6b). Similar differential regulation of *CAS*, *BAS* and *LS* was reported in *W. somnifera* cell cultures treated with different elicitors such as MeJA, gibberellic acid and yeast extract (Dhar *et al.*, 2014). Moreover, *W. somnifera* BAS (K_m, 38.48 μM) exhibited approximately 2.6-fold lower K_m than CAS (K_m, 99.51 μM) for 2,3-oxidosqualene (Dhar *et al.*, 2014), suggesting

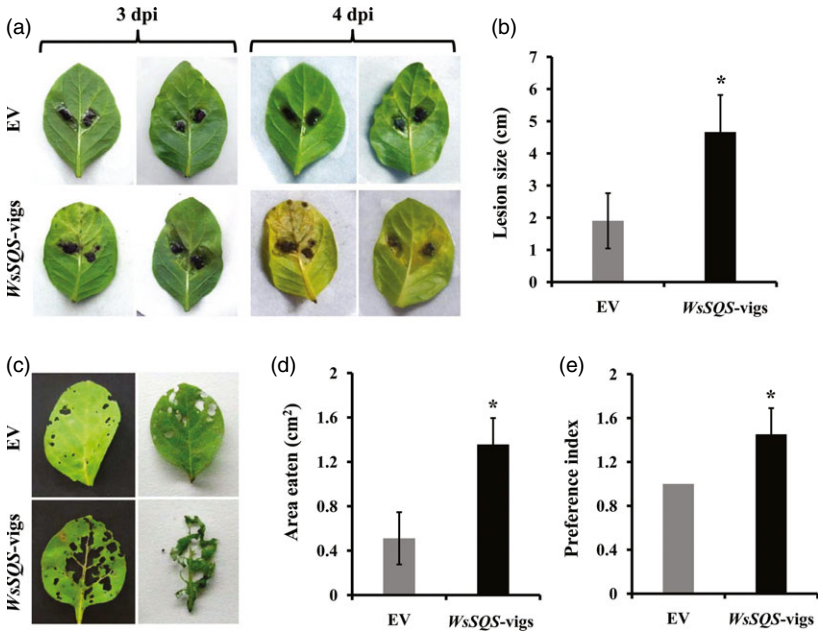

Figure 9 *Botrytis cinerea* infection and tobacco cutworm feeding assays on EV and *WsSQS*-vigs leaves of *Withania somnifera*. (a) Phenotype of *B. cinerea* infection on detached leaves on 3 and 4 days after treatment. Infection assay was carried out using fully expanded leaves having viral phenotype at 30 dpi. Excised leaves were inoculated with 20-μL drop of *B. cinerea* spore suspension (approximately 10^5 spores/mL) at the centre of abaxial side and kept at 23 °C with high humidity. (b) Statistical data of lesion size 4 days after treatment. For lesion size, the data are means ± SE of two independent experiments representing five biological replicates. Asterisk indicates a significant difference from the control (Student's *t*-test; $*P < 0.05$). (c) Dual-choice feeding preference assay of EV and *WsSQS*-vigs leaves using tobacco cutworm (*Spodoptera litura*). Equal numbers of second-instar cutworm (six each) were placed on EV and *WsSQS*-vigs leaves, and area fed was recorded after 12 h. (d) Leaf area eaten by *S. litura* in *WsSQS*-vigs leaves compared with EV leaves and corresponding preference index (PI) (e). Data represent means ± SE of two independent experiments representing six biological replicates. Asterisk indicates a significant difference from the control (Student's *t*-test; $*P < 0.05$).

that β-amyrin biosynthesis would still continue as BAS has higher affinity while the competing CAS has less chance to catalyse cycloartenol formation with its low affinity under reduced 2,3-oxidosqualene levels in *WsSQS*-vigs plants. Thus, increased β-amyrin and decreased cycloartenol derived from the common precursor pool of 2-3 oxidosqualene in *WsSQS*-silenced *W. somnifera* might be due to the combined effect of both differential mRNA levels and K_m of corresponding genes and enzymes, respectively. It is known that pentacyclic triterpenes present in surface waxes on leaves and fruits of various species are induced in response to biotic and abiotic stresses (cf. Stiti and Hartmann, 2012). Induction of β-amyrin synthase and β-amyrin content in *WsSQS*-vigs plants (Figure 6b) might be due to reduced phytosterols, which could have altered the membrane architecture to mimic the biotic stress signalling thereby alerting the system to produce more of these compounds.

SQS-silenced plants showed reduced levels of campesterol, sitosterol and stigmasterol (Figure 7) indicating correlation with decreased withanolides (Figure 4). This was in agreement with a recent report in which withanolides were enhanced upon feeding of these three phytosterols in *W. somnifera* leaves (Singh *et al.*, 2014). However, there was no effect on the level of cholesterol due to *WsSQS*-vigs in *W. somnifera* suggesting that cholesterol might not contribute to withanolides biosynthesis. Our observation was further supported by the fact that feeding of cholesterol did not affect withanolides accumulation in *W. somnifera* leaves (Singh *et al.*, 2014) and suspension cultures (Sivanandhan *et al.*, 2014). The higher degree of reduction of total withanolides (54%) as compared to total phytosterols (16%) in *WsSQS*-vigs plants tempts us to suggest that *SQS* silencing could also have down-regulated the genes involved in downstream withanolide pathway steps.

Although the role of SQS in biotic stress response was reported in other plants species (Devarenne *et al.*, 2002; Wang *et al.*, 2012b), the effect of SQS down-regulation on defence-related genes has not been investigated. Here, we report that *SQS* silencing led to drastic reduction of SA-dependent *PR1* and *PR5* (thaumatin) and JA-dependent *PR3* (chitinase) expression (Figure 8a). This was consistent with the observation that *WsSQS* was induced in response to both MJ and SA treatment in *W. somnifera* (Figure S13). It is known that biotrophic pathogens such as *P. syringae* and necrotrophic *B. cinerea* infection stimulate the SA- and JA-dependent defence responses, respectively (Spoel *et al.*, 2007; Wang *et al.*, 2012a). This suggested that *SQS* silencing could also affect defence signalling. It is possible that reduced phytosterols due to *SQS* silencing might have altered the sterol homoeostasis resulting in altered fluidity and permeability of plasma membrane thereby affecting the functions of membrane bound proteins such as enzymes, channels, receptors or other signalling components (Carland *et al.*, 2010; Heintz *et al.*, 2012; Schaller, 2004). To check this hypothesis, we analysed the expression of *BR6OX2* involved in the production of brassinolide (BL), which has been shown to induce the expression of *PR* genes (Divi *et al.*, 2010) and acts as a positive regulator of cotton resistance against *Verticillium dahliae* (Gao *et al.*, 2013). *WsSQS*-vigs plants showed drastic reduction in *BR6OX2* mRNA levels (Figure 8b), suggesting possible reduction in endogenous BR levels. Moreover, *NPR1*, a master regulator of *PR* genes (Fan and

Dong, 2002), and its paralogue *NPR3* (Fu *et al.*, 2012) were also drastically reduced in *WsSQS*-vigs plants (Figure 8b). The fact that *NPR1* is not required for brassinolide-mediated induction of *PR1* expression (Divi *et al.*, 2010) and our observation that *BR6OX2*, *NPR* and *PR* were all down-regulated in *SQS*-silenced plants point to a brassinosteroid-independent phytosterol-mediated defence signalling, thus affecting biotic stress tolerance. These observations were further supported by reduced tolerance of *WsSQS*-vigs plants to bacteria *P. syringae* and fungus *B. cinerea* (Figures 8c and 9a,b). Furthermore, reduced levels of withanolides could have contributed to the decreased tolerance of *WsSQS*-vigs leaves to bacterial and fungal pathogens as withanolides have shown to possess antibacterial and antifungal properties (Choudhary *et al.*, 1995). *WsSQS*-vigs leaves also showed susceptibility to tobacco cutworm (Figure 9c). The drastic reduction of total withanolides (including withaferin A, withanolide IV and withanolide A) (Figure 4) would have resulted in reduced tolerance of *WsSQS*-vigs leaves to cutworm feeding (Figure 9c,d) as withanolides have antifeedant properties against herbivorous insects (Waiss *et al.*, 1993). Additionally, reduced *NPR1* expression may also have contributed to the reduced tolerance of *WsSQS*-vigs plants to cutworm feeding. Indeed, it was reported that *NPR1*-silenced *Nicotiana attenuata* plants were more susceptible to *Spodoptera exigua* larvae, suggesting NPR1's role in mediating herbivore resistance in plants (Rayapuram and Baldwin, 2007).

In conclusion, we have demonstrated that VIGS can be effectively utilized for assessing gene functions in *W. somnifera* by silencing *PDS* and *SQS*. Our results from *SQS*-silencing studies indicated a multilevel regulation of the sterol pathway and defence-related genes, and thus pointing to a combinatorial effect of reduced levels of phytosterols, withanolides, and *BR6OX2* and *NPR*-mediated *PR* gene expression leading to decreased biotic stress tolerance in *WsSQS*-vigs plants rather than the individual effect. As not much is known on the candidate genes involved in the biosynthesis of withanolides, the 'VIGS combined with withanolides analysis' approach presented in this study will greatly facilitate the elucidation of withanolides pathway in *W. somnifera* by utilizing the recently released transcriptome database (Gupta *et al.*, 2013) as well as the genome sequence data to be released by SOL genomics network.

Experimental procedures

Plant materials

Withania somnifera cv. Poshita (National Gene Bank, CSIR-CIMAP, India) seeds were germinated in plastic pots containing soil mixture. Seedlings were transplanted into trays of 25 pots at 2-leaf stage. After a week, when plants reached 4-leaf stage, agroinfiltration was carried out, and after infiltration, plants were grown in green house at 22–25 °C with 16 h light and 8 h dark.

RNA isolation, cDNA synthesis and qPCR analysis

RNA isolation, cDNA synthesis and qPCR analysis were performed as reported previously (Rai *et al.*, 2013; Rastogi *et al.*, 2014). For semi-quantitative RT-PCR, *18S rRNA* gene served as an endogenous control for RNA quantity. Real-time qPCR was performed using a linear range of cDNA and specific primers for each gene (Table S1) with Power SYBR_Green PCR Master Mix (Applied Biosystems, Foster City, CA) and run in ABI7900HT. Real-time qRT-PCR conditions were as follows: 94 °C for 10 min for one cycle, followed by 40 cycles of 94 °C for 15 s and 60 °C for 1 min. A final dissociation step was carried out to assess the quality of amplified product. Fold change differences in gene expression were analysed using the comparative cycle threshold (C_t) method (Applied Biosystems).

Gene cloning and construction of VIGS vectors

The pTRV1, pTRV2 and pTRV2-*NtPDS* vectors (described in Liu *et al.*, 2002b) procured from TAIR (www.arabidopsis.org) were used in this study. *WsPDS* and *WsSQS* gene fragments were amplified using gene-specific primers (Table S1) and cloned into pJET1.2 vector (Fermentas, Vilnius, Lithuania), and sequences were confirmed by nucleotide sequencing using an ABI 3130 Genetic Analyzer (Applied Biosystems). Confirmed gene fragments were cloned into pTRV2 vector to form pTRV2-*WsPDS* and pTRV2:*WsSQS* constructs (Figure S2).

Agrobacterium infiltration

Agrobacterium tumefaciens strain GV3101 was transformed with pTRV1, pTRV2 and pTRV derived constructs by the freeze–thaw method. *Agrobacterium* cultures were grown as described by Liu *et al.* (2002a). The bacterial cultures were harvested by centrifugation and resuspended in infiltration buffer [10 mM $MgCl_2$; 10 mM 2-(4-morpholino)-ethane sulfonic acid (MES); 200 μM acetosyringone pH 5.6] to obtain a 1.3 optical density and incubated at room temperature for 5–6 h. For leaf infiltration, mixture of *Agrobacterium* cultures containing 1 : 1 ratio of TRV1 and TRV2 or its derivatives was infiltrated using 1-mL needleless syringe on the abaxial side of leaves in 4-leaf-staged plants. For vacuum infiltration, *W. somnifera* plants were vacuum-infiltrated following the manner as described by Hileman *et al.* (2005). For sprouting, seeds were incubated with shaking (100 r.p.m./min) at 25 °C for 24 h and then were transferred to a Petri dish containing moist filter paper. The germinating sprouts were vacuum-infiltrated following the method as described by Yan *et al.* (2012). Postinfiltration plants/sprouts were kept in dark for overnight and then shifted to growth room that was maintained at 23–24 °C. First pair of newly emerged, fully expanded leaves having typical viral infection symptoms was collected from syringe-infiltrated plants 30 dpi and stored at −80 °C until further analysis.

Extraction of squalene, β-amyrin, phytosterols and withanolides from *Withania somnifera* leaves

Squalene, β-amyrin and total withanolides were extracted from 20 mg of *W. somnifera* dried leaf tissue according to Qin *et al.* (2010). The samples were run on TLC plates (silica gel 60 F_{254}; Merck, Darmstadt, Germany) using hexane : chloroform (92 : 8, v/v) solvent system for squalene hexane : acetone (80 : 20, v/v) solvent system for β-amyrin. The TLC plates were stained with iodine vapour, and the corresponding spots of squalene and β-amyrin were quantified by ImageJ 1.47 software (Schneider *et al.*, 2012). For withanolides analysis, the dried residue from above extraction was dissolved in methanol and analysed by HPLC (model: LC2010CHT; Shimadzu, Kyoto, Japan) containing a Phenomenex Luna 5μ C-18 (250 mm × 4.60 mm, 5 μm) column. The two solvents used for the analysis consisted of 1.02 mM of anhydrous potassium dihydrogen orthophosphate (KH_2PO_4) containing 0.05% orthophosphoric acid (solvent A) and acetonitrile (solvent B). Gradient programming of the solvent system was carried out initially at 95% A, then changed to 55% A and 20% A at 18.0 and 25.0 min, respectively. A total of 20% A was maintained for next 10 min, increased to 55% A at 35 min,

followed by 95% at 40 min that was maintained till the run time reached 45 min. The flow rate was set at 1.5 mL/min with UV detector wavelength of 227 nm. All standards of withanolides were from Natural Remedies (Bangalore, India). Twenty mirolitre of standards and samples was injected for analysis. Phytosterol extraction and GC analysis was carried out as was described previously using 100 mg of dried leaves (Singh *et al.*, 2014). All reference molecules used in GC were purchased from Sigma-Aldrich, St. Louis, MO.

Bacterial growth curve assay

P. syringae cultures were grown overnight at 28 °C with shaking in 5 mL of nutrient broth medium. The bacterial cultures were harvested by centrifugation and resuspended in 10 mM $MgCl_2$ and 0.01% Silwet to a final OD_{600} of 0.2 corresponding to 1×10^8 cfu/mL. *P. syringae* suspension was inoculated into the first-pair leaves of *WsSQS*-vigs and EV plants at 30 dpi having viral infection phenotype by infiltration using a needleless syringe and covered with transparent lids. Leaf discs were harvested 4 days after inoculation and ground in 10 mM $MgCl_2$. The cfu/cm^2 was determined by plating serial dilutions of leaf extracts on Pseudomonas-specific agar plates.

Fungal infection assay

Botrytis cinerea was cultured on Potato Dextrose Agar medium and incubated at 23 °C for 3 weeks. Spores were washed off from the medium using sterile water, and spore count was calculated by haemocytometer. *B. cinerea* infection assay was performed on detached fully expanded first-pair leaves of *WsSQS*-vigs and EV plants 30 days after TRV infection using 20 μL per drop of spore suspension (approximately 10^5 spores/mL). Inoculated leaves were kept at 23 °C under a transparent cover to maintain high humidity. The diameters (width) of fungal lesions on inoculated leaves were measured after 3–4 days.

Insect feeding assay

Spodoptera litura eggs were incubated at 25 °C in sterile Petri dishes until hatching. The larvae were fed on leaves of *Ricinus communis* before use in the experiments. For dual-choice feeding preference tests, fully expanded first-pair leaves with typical viral infection symptoms were detached from *WsSQS*-vigs and EV plants and placed on top of moist Whatman filter paper in a Petri dish. Second-instar larvae were starved for 4 h, and equal number (six each) of larvae were placed on each leaf. The eaten area was measured 12 h after the start of the experiment to calculate the feeding PI, where $PI = 2\ T/(T + C)$ (Kogan, 1972), and T and C are the areas eaten in silenced and control leaves, respectively.

Statistical analysis

Mean, standard error and number of replicates were used for statistical evaluation using GraphPad QuickCalc online software (http://www.graphpad.com/quickcalcs/ttest1.cfm). The statistical significance of differences between control and treated samples was tested by unpaired Student's *t*-test.

Acknowledgements

This work was supported by the TFYP project (BSC0203) of CSIR-Central Institute of Medicinal and Aromatic Plants. DAN thanks the Department of Biotechnology, Government of India, for the Ramalingaswami Fellowship (BT/HRD/35/24/2006). A.K.S. and A.R. are the recipients of a Research Fellowship from the Council of Scientific and Industrial Research (CSIR) and the University Grants Commission (UGC), respectively. The authors express their sincere gratitude to the Director, CSIR-CIMAP. The authors are grateful to Prof. Thomas Bach and Dr. Anthony Qualley for their suggestions and critical comments to improve the manuscript. HPLC service by Natural Remedies Pvt. Ltd., Bangalore, India, is also acknowledged.

Conflict of interest

The author declares no conflict of interest.

References

Carland, F., Fujioka, S. and Nelson, T. (2010) The sterol methyltransferases SMT1, SMT2, and SMT3 influence *Arabidopsis* development through nonbrassinosteroid products. *Plant Physiol.* **153**, 741–756.

Chaurasiya, N.D., Sangwan, N.S., Sabir, F., Misra, L. and Sangwan, R.S. (2012) Withanolide biosynthesis recruits both mevalonate and DOXP pathways of isoprenogenesis in Ashwagandha *Withania somnifera* L. (Dunal). *Plant Cell Rep.* **31**, 1889–1897.

Choudhary, I.M., Parveen, Z., Jabbar, A. and Ali, I. (1995) Antifungal steroidal lactones from *Withania coagulance*. *Phytochemistry*, **40**, 1243–1246.

Devarenne, T.P., Ghosh, A. and Chappell, J. (2002) Regulation of squalene synthase, a key enzyme of sterol biosynthesis, in tobacco. *Plant Physiol.* **129**, 1095–1106.

Dhar, N., Rana, S., Razdan, S., Bhat, W.W., Hussain, A., Dhar, R.S., Vaishnavi, S., Hamid, A., Vishwakarma, R. and Lattoo, S.K. (2014) Cloning and functional characterization of three branch point oxidosqualene cyclases from *Withania somnifera* (L.) Dunal. *J. Biol. Chem.* **289**, 17249–17267.

Divi, U.K., Rahman, T. and Krishna, P. (2010) Brassinosteroid-mediated stress tolerance in *Arabidopsis* shows interactions with abscisic acid, ethylene and salicylic acid pathways. *BMC Plant Biol.* **10**, 151.

Faivre-Rampant, O., Gilroy, E.M., Hrubikova, K., Hein, I., Millam, S., Loake, G.J., Birch, P., Taylor, M. and Lacomme, C. (2004) Potato virus X-induced gene silencing in leaves and tubers of potato. *Plant Physiol.* **134**, 1308–1316.

Fan, W. and Dong, X. (2002) In vivo interaction between NPR1 and transcription factor TGA2 leads to salicylic acid-mediated gene activation in Arabidopsis. *Plant Cell*, **14**, 1377–1389.

Fu, Z.Q., Yan, S., Saleh, A., Wang, W., Ruble, J., Oka, N., Mohan, R., Spoel, S.H., Tada, Y., Zheng, N. and Dong, X. (2012) NPR3 and NPR4 are receptors for the immune signal salicylic acid in plants. *Nature*, **486**, 228–232.

Gao, W., Long, L., Zhu, L.F., Xu, L., Gao, W.H., Sun, L.Q., Liu, L.L. and Zhang, X.L. (2013) Proteomic and virus-induced gene silencing (VIGS) Analyses reveal that gossypol, brassinosteroids, and jasmonic acid contribute to the resistance of cotton to *Verticillium dahliae*. *Mol. Cell Proteomics*, **12**, 3690–3703.

Ginzberg, I., Thippeswamy, M., Fogelman, E., Demirel, U., Mweetwa, A.M., Tokuhisa, J. and Veilleux, R.E. (2012) Induction of potato steroidal glycoalkaloid biosynthetic pathway by overexpression of cDNA encoding primary metabolism HMG-CoA reductase and squalene synthase. *Planta*, **235**, 1341–1353.

Gupta, P., Goel, R., Pathak, S., Srivastava, A., Singh, S.P., Sangwan, R.S., Asif, M.H. and Trivedi, P.K. (2013) De novo assembly, functional annotation and comparative analysis of *Withania somnifera* leaf and root transcriptomes to identify putative genes involved in the withanolides biosynthesis. *PLoS ONE*, **8**, 62714.

Hahm, E.R., Moura, M.B., Kelley, E.E., Van Houten, B., Shiva, S. and Singh, S.V. (2011) Withaferin A-induced apoptosis in human breast cancer cells is mediated by reactive oxygen species. *PLoS ONE*, **6**, e23354.

Hasunuma, T., Takeno, S., Hayashi, S., Sendai, M., Bamba, T., Yoshimura, S., Tomizawa, K.-I., Fukusaki, E. and Miyake, C. (2008) Overexpression of 1-deoxy-D-xylulose-5-phosphate reductoisomerase gene in chloroplast

contributes to increment of isoprenoid production. *J. Biosci. Bioeng.* **105**, 518–526.

Heintz, D., Heintz, D., Gallien, S., Compagnon, V., Berna, A., Suzuki, M., Yoshida, S., Muranaka, T., Van Dorsselaer, A., Schaeffer, C., Bach, T.J. and Schaller, H. (2012) Phosphoproteome exploration reveals a reformatting of cellular processes in response to low sterol biosynthetic capacity in Arabidopsis. *J. Proteome Res.* **11**, 1228–1239.

Hileman, L.C., Drea, S., Martino, G., Litt, A. and Irish, V.F. (2005) Virus-induced gene silencing is an effective tool for assaying gene function in the basal eudicot species *Papaver somniferum* (opium poppy). *Plant J.* **44**, 334–341.

Holmberg, N., Harker, M., Gibbard, C.L., Wallace, A.D., Clayton, J.C., Rawlins, S., Hellyer, A. and Safford, R. (2002) Sterol C-24 methyltransferase type 1 controls the flux of carbon into sterol biosynthesis in tobacco seed. *Plant J.* **130**, 303–311.

Kaileh, M., Vanden Berghe, W., Heyerick, A., Horion, J., Piette, J., Libert, C., De Keukeleire, D., Essawi, T. and Haegeman, G. (2007) Withaferin A strongly elicits IκB kinase β hyperphosphorylation concomitant with potent inhibition of its kinase activity. *J. Biol. Chem.* **282**, 4253–4264.

Koduru, S., Kumar, R., Srinivasan, S., Evers, M.B. and Damodaran, C. (2010) Notch-1 inhibition by Withaferin-A: a therapeutic target against colon carcinogenesis. *Mol. Cancer Ther.* **9**, 202–210.

Kogan, M. (1972) Feeding and nutrition of insects associated with soybeans. Soybean resistance and host preferences of the Mexican bean beetle, *Epilachna varivestis*. *Ann. Entomol. Soc. Am.* **65**, 675–683.

Lee, M.H., Jeong, J.H., Seo, J.W., Shin, C.G., Kim, Y.S., In, J.G., Yang, D.C., Yi, J.S. and Choi, Y.E. (2004) Enhanced triterpene and phytosterol biosynthesis in *Panax ginseng* overexpressing squalene synthase gene. *Plant Cell Physiol.* **45**, 976–984.

Li, R., Reed, D.W., Liu, E., Nowak, J., Pelcher, L.E., Page, J.E. and Covello, P.S. (2006) Functional genomic analysis of alkaloid biosynthesis in *Hyoscyamus niger* reveals a cytochrome P450 involved in littorine rearrangement. *Chem. Biol.* **13**, 513–520.

Liu, Y., Schiff, M. and Dinesh-Kumar, S.P. (2002a) Virus-induced gene silencing in tomato. *Plant J.* **31**, 777–786.

Liu, Y., Schiff, M., Marathe, R. and Dinesh-Kumar, S.P. (2002b) Tobacco *Rar1*, *EDS1* and *NPR1/NIM1* like genes are required for *N*-mediated resistance to tobacco mosaic virus. *Plant J.* **30**, 415–429.

Liu, H., Fu, D., Zhu, B., Yan, H., Shen, X., Zuo, J., Zhu, Y. and Luo, Y. (2012) Virus-induced gene silencing in eggplant (*Solanum melongena*). *J. Integr. Plant Biol.* **54**, 422–429.

Martínez, I.M. and Chrispeels, M.J. (2003) Genomic analysis of the unfolded protein response in Arabidopsis shows its connection to important cellular processes. *Plant Cell*, **15**, 561–576.

Mirjalili, M.H., Moyano, E., Bonfill, M., Cusido, R.M. and Palazón, J. (2009) Steroidal lactones from *Withania somnifera*, an ancient plant for novel medicine. *Molecules*, **14**, 2373–2393.

Moses, T., Pollier, J., Thevelein, J.M. and Goossens, A. (2013) Tansley review bioengineering of plant (tri)terpenoids: from metabolic engineering of plants to synthetic biology *in vivo* and *in vitro*. *New Phytol.* **200**, 27–43.

Nagegowda, D.A. (2010) Plant volatile terpenoid metabolism: biosynthetic genes, transcriptional regulation and subcellular compartmentation. *FEBS Lett.* **584**, 2965–2973.

Nes, W.D. and Venkatramesh, M. (1999) Enzymology of phytosterol transformations. *Crit. Rev. Biochem. Mol. Biol.* **34**, 81–93.

Phillips, D.R., Rasbery, J.M., Bartel, B. and Matsuda, S.P.T. (2006) Biosynthetic diversity in plant triterpene cyclization. *Curr. Opin. Plant Biol.* **9**, 305–314.

Qin, B., Eagles, J., Mellon, F.A., Mylona, P., Peña-Rodriguez, L. and Osbourn, A.E. (2010) High throughput screening of mutants of oat that are defective in triterpene synthesis. *Phytochemistry*, **71**, 1245–1252.

Rai, A., Smita, S.S., Singh, A.K., Shanker, K. and Nagegowda, D.A. (2013) Heteromeric and homomeric geranyl diphosphate synthases from *Catharanthus roseus* and their role in monoterpene indole alkaloid biosynthesis. *Mol. Plant*, **6**, 1531–1549.

Rastogi, S., Meena, S., Bhattacharya, A., Ghosh, S., Shukla, R.K., Sangwan, N.S., Lal, R.K., Gupta, M.M., Lavania, U.C., Gupta, V., Nagegowda, D.A. and Shasany, A.K. (2014) *De novo* sequencing and comparative analysis of holy and sweet basil transcriptomes. *BMC Genomics*, **15**, 588–605.

Ratcliff, F., Martin-Hernandez, A.M. and Baulcombe, D.C. (2001) Tobacco rattle virus as a vector for analysis of gene function by silencing. *Plant J.* **25**, 237–245.

Rayapuram, C. and Baldwin, I.T. (2007) Increased SA in *NPR1*-silenced plants antagonizes JA and JA-dependent direct and indirect defenses in herbivore-attacked *Nicotiana attenuata* in nature. *Plant J.* **52**, 700–715.

Schaller, H. (2004) New aspects of sterol biosynthesis in growth and development of higher plants. *Plant Physiol. Biochem.* **42**, 465–476.

Schneider, C.A., Rasband, W.S. and Eliceiri, K.W. (2012) NIH image to ImageJ: 25 years of image analysis. *Nat. Methods*, **9**, 671–675.

Sehgal, N., Gupta, A., Valli, R.K., Joshi, S.D., Mills, J.T., Hamel, E., Khanna, P., Jain, S.C., Thakur, S.S. and Ravindranath, V. (2012) *Withania somnifera* reverses Alzheimer's disease pathology by enhancing low-density lipoprotein receptor-related protein in liver. *Proc. Natl Acad. Sci. USA*, **109**, 3510–3515.

Senthil-Kumar, M., Hema, R., Anand, A., Kang, L., Udayakumar, M. and Mysore, K.S. (2007) A systematic study to determine the extent of gene silencing in *Nicotiana benthamiana* and other Solanaceae species when heterologous gene sequences are used for virus-induced gene silencing. *New Phytol.* **176**, 782–791.

Seo, J.W., Jeong, J.H., Shin, C.G., Lo, S.C., Han, S.S., Yu, K.W., Harada, E., Han, J.Y. and Choi, Y.E. (2005) Overexpression of squalene synthase in *Eleutherococcus senticosus* increases phytosterol and triterpene accumulation. *Phytochemistry*, **66**, 869–877.

Singh, S., Pal, S., Shanker, K., Chanotiya, C.S., Gupta, M.M., Dwivedi, U.N. and Shasany, A.K. (2014) Sterol partitioning by HMGR and DXR for routing intermediates toward withanolide biosynthesis. *Physiol. Plant.* **152**, 617–633.

Sivanandhan, G., Selvaraj, N., Ganapathi, A. and Manickavasagam, M. (2014) Enhanced biosynthesis of withanolides by elicitation and precursor feeding in cell suspension culture of *Withania somnifera* (L.) Dunal in shake-flask culture and bioreactor. *PLoS ONE*, **9**, 104005.

Spoel, S.H., Johnson, J.S. and Dong, X. (2007) Regulation of tradeoffs between plant defenses against pathogens with different lifestyles. *Proc. Natl Acad. Sci. USA*, **104**, 18842–18847.

Stiti, N. and Hartmann, M.A. (2012) Nonsterol triterpenoids as major constituents of *Olea europaea*. *J. Lipids*, **2012**, 476595.

Waiss, A.C., Elliger, C.A. and Benson, M. (1993) Insect inhibitory lactone glucosides of *Physalis peruviana*. *Nat. Prod. Lett.* **2**, 115–118.

Wang, H., Nagegowda, D.A., Rawat, R., Bouvier-Navé, P., Guo, D., Bach, T.J. and Chye, M.L. (2012a) Overexpression of *Brassica juncea* wild-type and mutant HMG-CoA synthase 1 in *Arabidopsis* up-regulates genes in sterol biosynthesis and enhances sterol production and stress tolerance. *Plant Biotechnol. J.* **10**, 31–42.

Wang, K., Senthil-Kumar, M., Ryu, C.M., Kang, L. and Mysore, K.S. (2012b) Phytosterols play a key role in plant innate immunity against bacterial pathogens by regulating nutrient efflux into the apoplast. *Plant Physiol.* **158**, 1789–1802.

Wentzinger, L.F., Bach, T.J. and Hartmann, M.A. (2002) Inhibition of squalene synthase and squalene epoxidase in tobacco cells triggers an up-regulation of 3-hydroxy-3-methylglutaryl coenzyme a reductase. *Plant Physiol.* **130**, 334–346.

Yan, H., Fu, D., Zhu, B., Liu, H., Shen, X. and Luo, Y. (2012) Sprout vacuum-infiltration, a simple and efficient agroinoculation method for virus-induced gene silencing in diverse solanaceous species. *Plant Cell Rep.* **31**, 1713–1722.

Supporting information

Additional Supporting information may be found in the online version of this article:

Figure S1 Confirmation of TRV infection in *Withania somnifera* by RT-PCR analysis.
Figure S2 pTRV derived construct maps used in this study.
Figure S3 The frequency and effectiveness of *PDS* gene silencing in *Withania somnifera*.

Figure S4 Phenotype of representative EV and TRV:*WsSQS* infiltrated plants.
Figure S5 Analysis of squalene content in *EV* and *SQS*-silenced *Withania somnifera* plants.
Figure S6 Effect of squalestatin treatment on withanolides in *Withania somnifera* leaves.
Figure S7 Chlorophyll and carotenoid content of EV and *WsSQS*-vigs leaves.
Figure S8 Relative expression levels of selected MEP, MVA, and triterpenoid pathway genes in control (water) and squalestatin-treated leaves.
Figure S9 Analysis of β-amyrin content in *EV* and *SQS*-silenced *Withania somnifera* plants.
Figure S10 Relative quantification of β-amyrin contents of control (water) and squalestatin-treated plants.
Figure S11 Sequence alignment of *PDS* gene sequences from *Withania somnifera* and *N. tabacum*.
Figure S12 Silencing of *Withania somnifera* endogenous *PDS* using the heterologous *N. tabacum PDS* gene sequence.
Figure S13 Relative expression levels of *WsSQS* in Methyl jasmonate (MeJA)- and salicin-treated *Withania somnifera* leaves.
Table S1 List of primers used in this study.

